Orclever Proceedings of Research and Development
https://doi.org/10.56038/oprd.v5i1.513
OR CLEVER Science & Research Group

Conference Article

Mixing Performance Analysis of a Planetary Concrete Mixer

Jaber Salamat[1*], Bülent Genç[2*], Metin Aydogdu[3*]

[1] Mechanical Engineering Department, Istanbul Technical University, 34437 Istanbul, Turkey,
Orcid ID: https://orcid.org/0000-0003-0491-745X, E-mail: salamat@itu.edu.tr,
[2] Elkon Concrete Batching Plants, R&D Center, 59510 Tekirdag, Turkey,
Orcid ID: https://orcid.org/0000-0001-8093-808X, E-mail: bulent.genc@elkon.net,
[3] Mechanical Engineering Department, Trakya University, 22030 Edirne, Turkey,
Orcid ID: https://orcid.org/0000-0003-4567-2532, E-mail: metina@trakya.edu.tr,
* Correspondence: salamat@itu.edu.tr

Received 15 October 2024
Received in revised form 21 December 2024
In final form 22 December 2024

4th International Conference on Design, Research and Development (RDCONF 2024)
December 19 - 20, 2024

Reference: Salamat, J., Genç, B., & Aydogdu, M. (2024). Mixing performance analysis of a planetary concrete mixer. Orclever Proceedings of Research and Development, 5(1), 186-196.

Abstract

In this research, the discrete element method is employed to study the mixing performance of a $1m^3$ *capacity planetary concrete mixer. The performance was evaluated based on the homogeneity of granular particle mixing and the scanning of the mixer's inside by the gyrational and planetary mixing blades. The granular particle mixing was realized by applying the Hertz-Mindlin contact law, constant directional torque, and the Simplified Johnson-Kendall-Roberts (SJKR) models using open-source software. Furthermore, analytical formulations for the trajectories of mixing blades were developed and implemented in MATLAB. The trajectories were plotted at various time intervals, and it was observed that the entire mixer was fully scanned in approximately 30 seconds. Finally, numerical and analytical results were compared to verify the findings.*

Keywords: *Discrete Element Method (DEM), Planetary Concrete Mixer, Granular Particles, Mixing Blades*

https://doi.org/10.56038/oprd.v5i1.513

1. Introduction

Fresh concrete is ubiquitous in the construction industry. The performance of high-quality concrete is primarily influenced by the homogeneous mixing of its constituent ingredients. To achieve this quality, numerous concrete mixing machines have been designed, developed, and mass produced to facilitate the preparation of fresh concrete for civil engineering projects. These machines can be broadly categorized into two main types: vertical rotating machines, such as pan mixers and planetary mixers, and horizontal rotating machines, including twin-shaft mixers, continuous mixers, ribbon mixers, and others. Referring to previous research on concrete mixing, relatively few studies have focused on the numerical simulation of concrete mixing using planetary mixers. This highlights a significant gap in the literature, emphasizing the need for further study and analysis of the mixing dynamics and efficiency of planetary mixers using computational methods.

Valigi et al. [1] developed a dynamic simulation environment to predict the behavior and service life of planetary concrete mixers by analyzing their geometric and physical parameters. Cazacliu [2] investigated the relationship between the evolution of the microstructure of concrete materials and the mixing power in a planetary mixer. Valigi et al. [3,4] also studied the wear resistance of mixing blades in planetary concrete mixers and proposed structurally modified blades to enhance durability against wear. Long et al. [5] characterized the mixing performance and power consumption of a twin-blade planetary mixer with non-cohesive particles using the Discrete Element Method (DEM). Zheng et al. [6] examined the planetary mixer from a kinematics perspective and proposed a digital evaluation method for analyzing the mixing efficiency of the planetary arm. Additionally, Salamat and Genç analyzed the mixing performance of two different agitator units in a planetary concrete mixer using DEM [7].

In this study, the Discrete Element Method (DEM) was utilized to analyze the mixing performance of a $1m^3$ capacity planetary concrete mixer. Statistical methods were applied to calculate the mixing degree over one complete cycle. The Lacey and Miles methods [8] were employed to calculate the mixing degree, and the results provided quantitative data about the homogeneity of the mixture inside the planetary mixer. Additionally, mathematical formulations for the trajectories of the mixing blades were developed and plotted at various time intervals using MATLAB. The results from the numerical analysis were compared with those from analytical analysis to validate the findings. Numerical simulations were conducted using LIGGGHTS 3.0, an open-source DEM particle simulation software. LIGGGHTS stands for "LAMMPS Improved for General Granular and Granular Heat Transfer Simulations" and is based on LAMMPS

https://doi.org/10.56038/oprd.v5i1.513

("Large Atomic and Molecular Massively Parallel Simulator"), an open-source molecular dynamics code developed by Sandia National Laboratories for massively parallel computing on distributed memory machines [9,10].

2. Materials and Methods

2.1. Mathematical Model for DEM Analysis

DEM is a mathematical model used to analyze the dynamics of granular materials and particulate systems. It was first developed by Cundall and Strack [11] to analyze the trajectories of spherical and disk-shaped particles. The translational and rotational motion of each particle is described by the following equations:

$$m_i \frac{d\vec{V}_i}{dt} = \sum_{j=1}^{K_i} (\vec{F}^n_{c,ij} + \vec{F}^n_{d,ij} + \vec{F}^t_{c,ij} + \vec{F}^t_{d,ij}) + \sum_{j=1}^{N_i} (\vec{F}_{v,ij}) + m_i \vec{g} \quad (1)$$

$$I_i \frac{d\vec{\omega}_i}{dt} = \sum_{j=1}^{K_i} (\vec{T}^t_{ij} + \vec{T}^r_{ij}) \quad (2)$$

Where, m_i, I_i, $\vec{V}_i$, $\vec{\omega}_i$, K_i , N_i, and $\vec{g}$ denote the mass, moment of inertia, translational velocity, angular velocity, number of particles in contact with particle i, number of particles in the immediate neighborhood of particle i, and acceleration due to gravity, respectively. The contact and damping forces in the normal and tangential directions are represented by $\vec{F}^n_{c,ij}$, $\vec{F}^n_{d,ij}$, $\vec{F}^t_{c,ij}$ and $\vec{F}^t_{d,ij}$, sequentially. $\vec{F}_{v,ij}$ indicates the cohesive force between particles i and j. Furthermore, the tangential and rolling friction torques are denoted by $\vec{T}^t_{ij}$ and $\vec{T}^r_{ij}$ consecutively.

To study the mixing performance of planetary concrete mixers, the Hertz-Mindlin contact law, the constant directional torque model, and the SJKR contact model were implemented in the simulation using LIGGGHTS, an open-source DEM software. The SJKR model is a simplified Johnson-Kendall-Roberts (JKR) cohesion model, incorporating an additional normal force to simulate the cohesion between particles. Comprehensive mathematical formulations are provided in previous publication and related literature [12].

2.2. Physical Model and Simulation

As shown in Figure 1, the main mixing components of the planetary concrete mixer consist of a sidewall blade, a gyrational mixing blade, and two planetary mixing arms. Each planetary mixing arm is equipped with two mixing blades that rotate in a clockwise direction at 57.9 rpm while simultaneously revolving clockwise around the central point of the mixer at 16.2 rpm. Also, the sidewall and gyrational mixing blades rotate around

https://doi.org/10.56038/oprd.v5i1.513

the central point of the mixer at 16.2 rpm. The mixing blades are powered by an ELKON type planetary gearbox, which is specially designed for application in both stationary and mobile concrete batching plants.

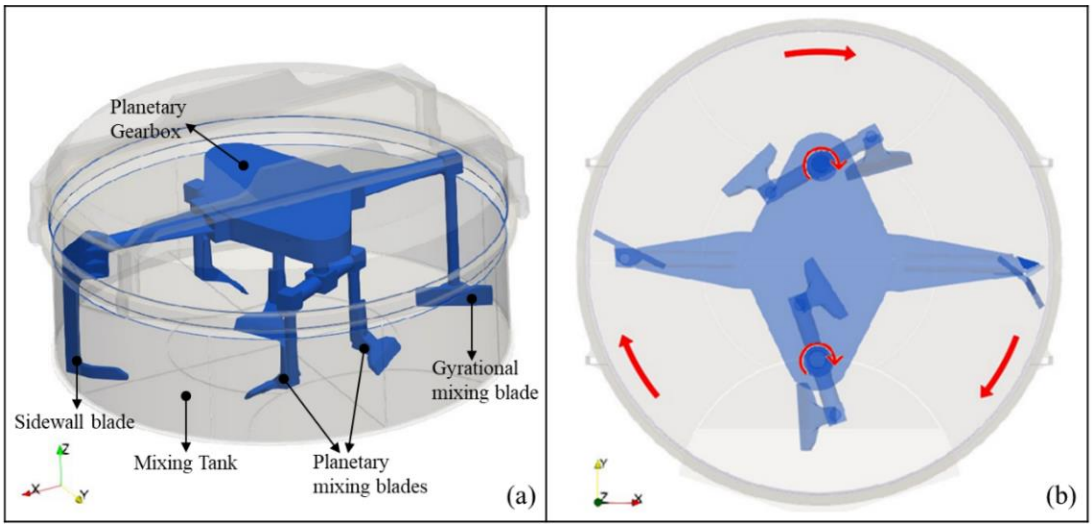

Figure 1. Geometric views of the planetary concrete mixer, (a) axonometric view, (b) top view.

The ANSYS SpaceClaim module was employed to construct the 3D geometries of the mixer components. The rotational speed of the mixer and its material properties were then defined within the simulation environment using User-Defined Function (UDF) codes, allowing for precise customization and control of the simulation parameters. Additionally, a minimum time step for reliable simulation was determined using the Rayleigh time step criterion [12]. Subsequently, two different colors of solid granular particles, each with specific physical and mechanical properties, were generated within the planetary concrete mixer, which enabled the analysis of particle behavior and mixing efficiency in the simulation. The input parameters used in the simulation are detailed in Table 1, providing a comprehensive overview of the setup conditions and employed properties.

Table 1: Properties of particles and walls used in DEM simulation.

Material Properties	**Particle**	**Wall**
Density(kg/m^3)	2400	7800
Radius (mm)	10	-
Young's Modulus (N/m^2)	10×10^6	210×10^9
Poisson Ratio	0.30	0.32
Contact Properties	**Particle-Particle**	**Particle-Wall**
Sliding Friction Coefficient	0.30	0.20
Rolling Friction Coefficient	0.10	0.01
Coefficient of Restitution	0.25	0.25
Cohesion (kJ/m^3)	100	100

https://doi.org/10.56038/oprd.v5i1.513

2.3. Blade's Kinematics

To evaluate the mixing efficiency of the mixer, the kinematic equations of the mixing blades were derived and plotted using MATLAB. Assuming B to be the central point of the single planetary blade, its instantaneous position is illustrated in Figure 2. The vectorial position of the blade in the fixed reference frame R can be written in the following form:

$$\overrightarrow{(OB)}_R = \overrightarrow{OA} + \overrightarrow{AO'} + \overrightarrow{O'B} \tag{3}$$

Considering the planetary motion of point B, which rotates clockwise around point A, while simultaneously revolving clockwise around the central point O (as shown in Figure 2), the following formulation can be written to describe the rotational and translational motion of point B [3].

$$\overrightarrow{(OA)}_R = \begin{cases} R_g.cos(\alpha_1) = R_g.cos(2\pi.N_g.t) \\ R_g.sin(\alpha_1) = R_g.sin(2\pi.N_g.t) \\ 0 \end{cases} \tag{4}$$

$$\overrightarrow{(AO')}_R = \begin{cases} 0 \\ 0 \\ \overrightarrow{AO'} \end{cases}, \quad \overrightarrow{(O'B)}_R = \begin{cases} R_p.cos(\alpha_2) = R_p.cos(2\pi.(N_g+N_p).t) \\ R_p.sin(\alpha_2) = R_p.sin(2\pi.(N_g+N_p).t) \\ 0 \end{cases} \tag{5}$$

$$\overrightarrow{(OB)}_R = \begin{cases} R_g.cos(2\pi.N_g.t) + R_p.cos(2\pi.(N_g+N_p).t) \\ R_g.sin(2\pi.N_g.t) + R_p.sin(2\pi.(N_g+N_p).t) \\ 0 \end{cases} \tag{6}$$

Here, α_1, α_2, R_g, R_p, N_g, and N_r represent the gyrational angle, planetary angle, radius of the gyrational motion, radius of the planetary motion, rotational speed of the gyrational motion (clockwise), and rotational speed of the planetary motion (clockwise), respectively. The instantaneous velocity vector of the point B can be obtained by differentiating the equation (6) with respect to time.

$$\left(\overrightarrow{V_B}\right)_R = \left(\frac{d\overrightarrow{OB}}{dt}\right)_R = \begin{cases} -2\pi R_g N_g.sin(2\pi.N_g.t) - 2\pi R_p(N_g+N_p).sin(2\pi.(N_g+N_p).t) \\ 2\pi R_g N_g.cos(2\pi.N_g.t) + 2\pi R_p(N_g+N_p).cos(2\pi.(N_g+N_p).t) \\ 0 \end{cases} \tag{7}$$

Therefore, the magnitude of velocity of point B is expressed as:

https://doi.org/10.56038/oprd.v5i1.513

$$\| \overrightarrow{V_B} \| = 2\pi \sqrt{(R_g N_g)^2 + {R_p}^2 (N_g + N_p)^2 + 2R_g R_p N_g (N_g + N_p) cos(2\pi N_p t)} \quad (8)$$

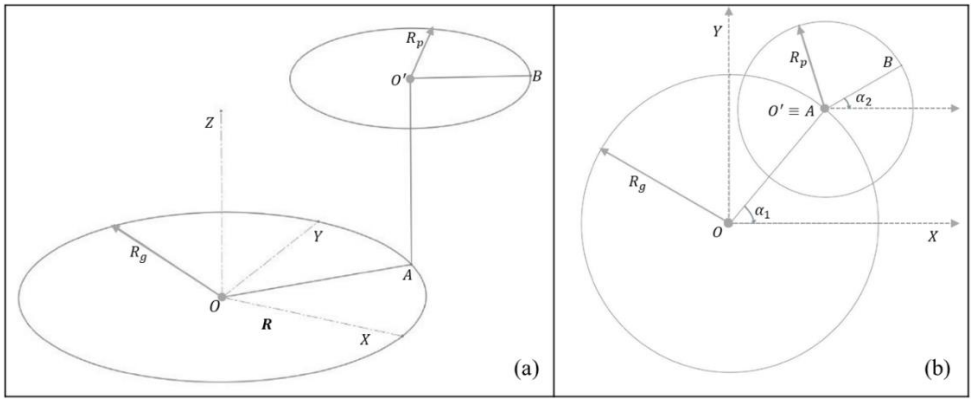

Figure 2. 3D kinematic scheme of a single planetary blade (a) and its projection on the horizontal (X-Y) plane (b) adapted from [3]

Equation (6) was extended to account for all blade categories within the planetary concrete mixer. This extension enabled the evaluation of the mixer's inside scanning capability, a critical measure of how effectively the blades cover the entire interior to achieve uniform mixing. The blade trajectories were plotted at different time instants, and it was observed that the entire mixer was fully scanned in approximately 30 seconds.

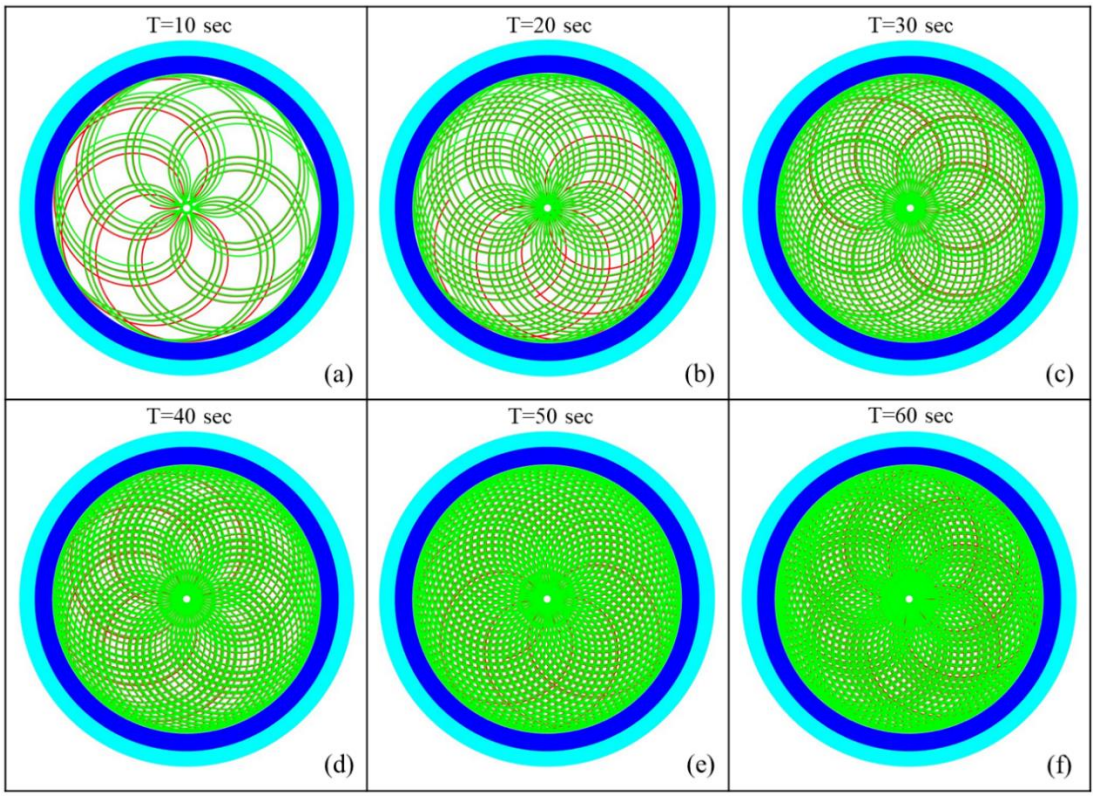

Figure 3. Plane trajectories of the mixing blades in planetary concrete mixer.

https://doi.org/10.56038/oprd.v5i1.513

3. Results and Discussion

In this mixing simulation, 200,000 monosized granular particles with an equal ratio of two different colors were injected into the $1m^3$ planetary concrete mixer under the influence of gravitational force. These particles are generated based on the physical and mechanical properties presented in Table 1. To model interactions between particles and between particles and the mixer body, the Hertz-Mindlin contact law and the constant directional torque model are employed. Furthermore, during the mixing stage, the SJKR model is utilized to simulate the cohesion of granular particles. The total simulation time is 60 seconds, comprising 4 seconds of simultaneous charging and mixing, followed by 56 seconds of pure mixing.

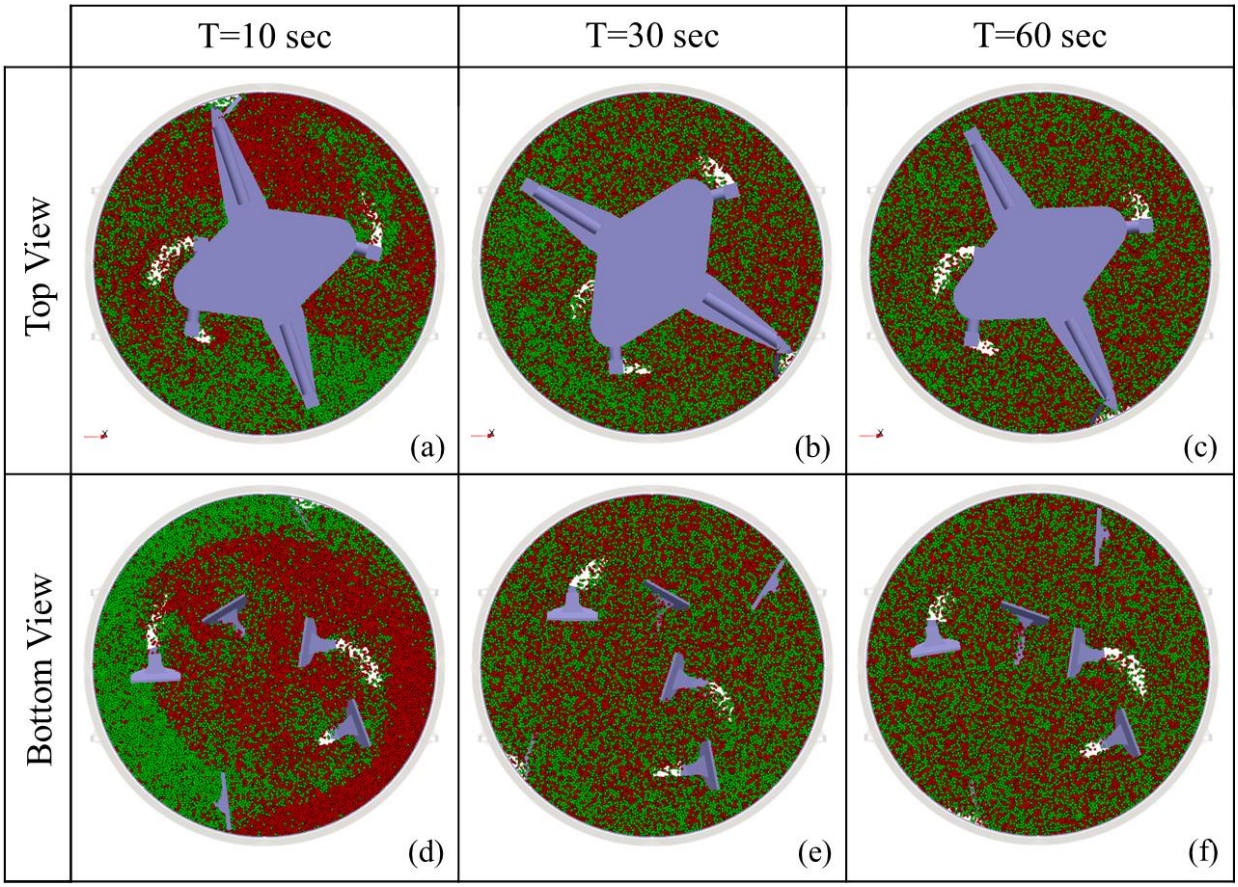

Figure 4. Comparison of particles mixing snapshots from the top and bottom views of planetary concrete mixer at different time instants.

Figures 4 presents a series of simulation snapshots from the top and bottom views of the planetary concrete mixer at various mixing times. These snapshots illustrate the progressive evolution of granular particle homogeneity achieved through different

https://doi.org/10.56038/oprd.v5i1.513

mixing mechanisms, such as convection, diffusion, and shearing. The results demonstrate the effectiveness of mixing over time, emphasizing a clear visualization of particle homogenization from an uneven mixture distribution in the early stages of mixing to a more homogeneous mixture as the mixing continues.

To quantitatively study the mixing homogeneity, twenty-one mixture samples were extracted from different mixer locations. The extracted sample numbers and size are big enough to cover the entire planetary mixer. The Lacey and Miles methods are utilized to calculate the mixing degree over one complete cycle, and the results are given in Figure 5. In this figure, the mixing degrees reach their maximum values after nearly 35 seconds of the mixing process and reach a steady state condition.

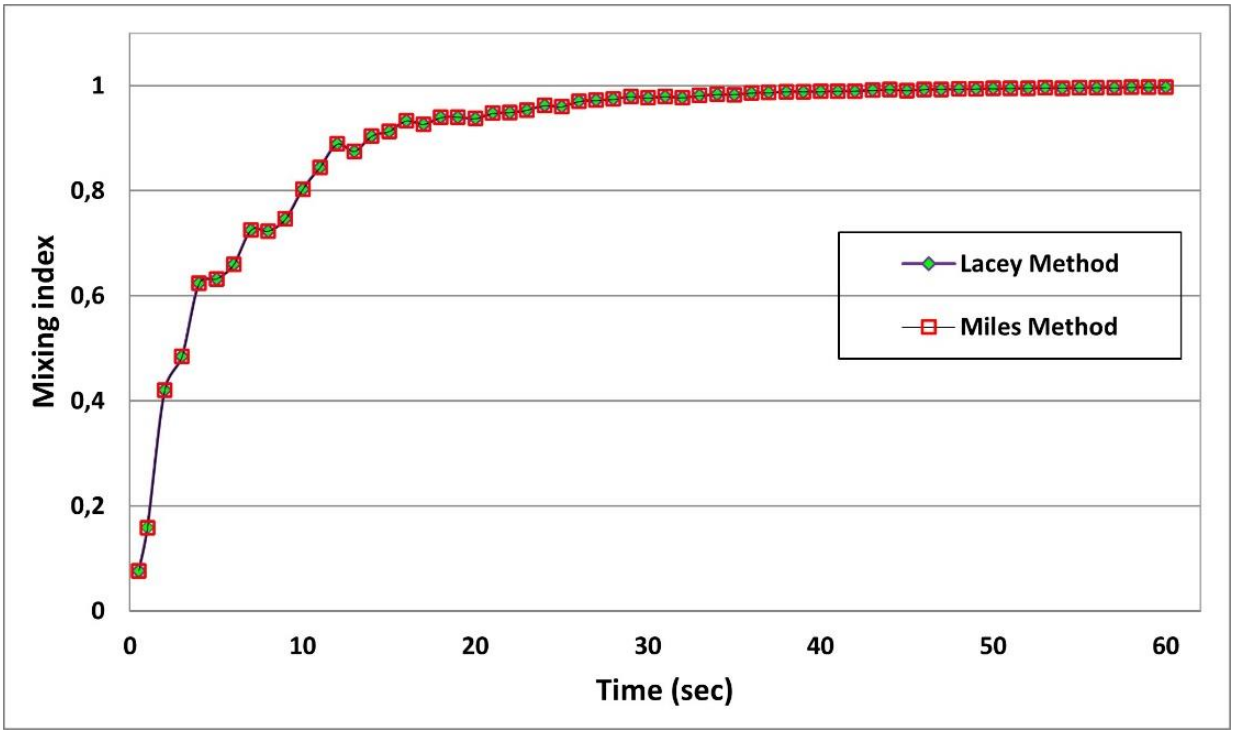

Figure 5. The mixing index versus time via two different statistical methods in the planetary concrete mixer.

To observe the particles' flow regimes, the velocity vectors of granular particles are given from the top and bottom views in Figure 6. The velocity values of granular particles around the planetary blades are greater than those of other mixing blades due to the rotational velocity difference. Also, the velocity flow regimes at the center of the mixer are lower than those in the sidewall region because the flow regimes from two planetary arms come to face at the center of the planetary concrete mixer.

https://doi.org/10.56038/oprd.v5i1.513

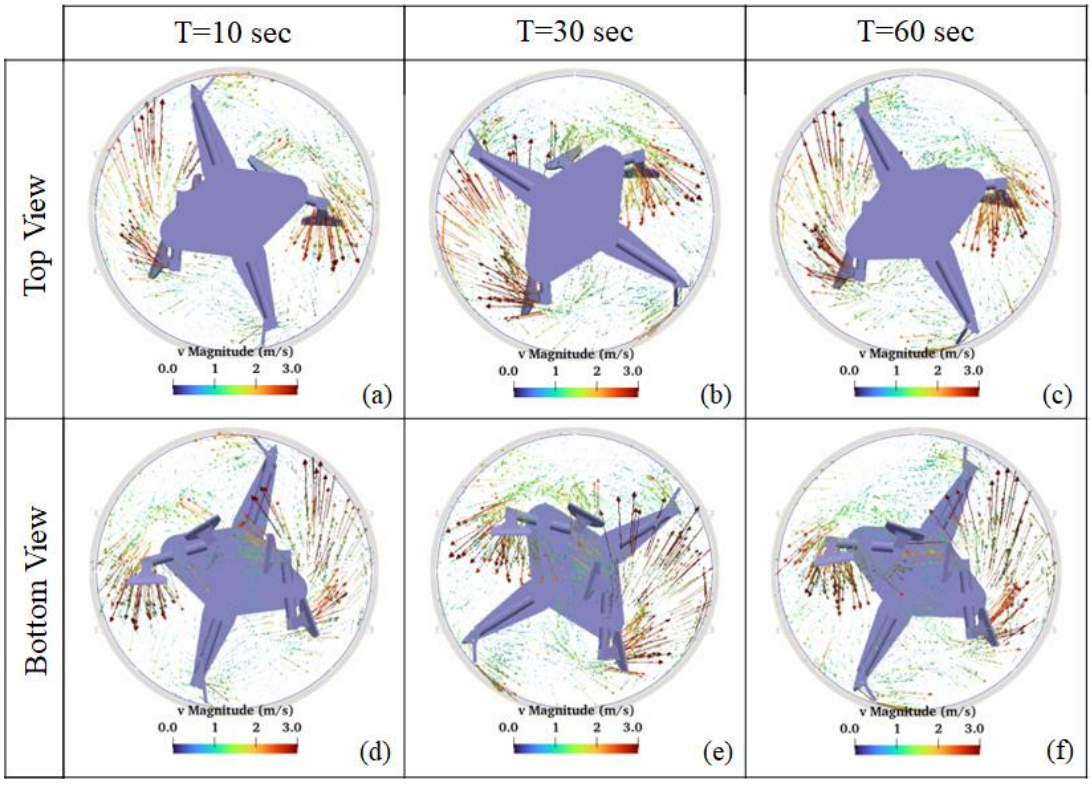

Figure 6. Comparison of simulation snapshots from velocity vectors of particles in various time instants.

4. Conclusions and Outlook

A numerical study based on DEM was realized to analyze the mixing performance of a $1m^3$ capacity planetary concrete mixer. The performance was evaluated based on the homogeneity of granular particle mixing on the minimum mixing time. On the other hand, analytical formulation was developed to analyze the trajectories of mixing blades. Then, mathematical equations were plotted using MATLAB to assess the coverage and scanning efficiency of the mixer's interior. By comparing the numerical and analytical results, the mixing degrees reach their maximum values after 35 seconds of the mixing process, and the full coverage with scanning capability of mixing blades completes approximately at the same time interval.

5. Acknowledgements

The author would like to thank the ELKON companies Chairman, Mr. Mustafa Alpagut, for funding this project with the grant number ELK24/03.

6. Abbreviations

DEM Discrete Element Method

https://doi.org/10.56038/oprd.v5i1.513

SJKR Simplified Johnson-Kendall-Roberts

7. Nomenclature

Latin Symbols

m_i	Mass, kg
I_i	Moment of inertia, kg. m^2
$\vec{g}$	Acceleration due to gravity, m. s^{-2}
$\vec{V}_i$	Translational velocity, m. s^{-1}
$\vec{F}^n_{c,ij}$	Contact force in the normal direction, N
$\vec{F}^n_{d,ij}$	Damping force in the normal direction, N
$\vec{F}^t_{c,ij}$	Contact force in the tangential direction, N
$\vec{F}^t_{d,ij}$	Damping force in the tangential direction, N
$\vec{F}_{v,ij}$	Cohesive force, N
$\vec{T}^t_{ij}$	Torques resulting from tangential force, N. m
$\vec{T}^r_{ij}$	Rolling friction torque, N. m
K_i	Number of particles in contact with particle i,
N_i	Number of particles in the immediate neighborhood of particle i,
R_g	Radius of the gyrational motion, m
R_p	Radius of the planetary motion, m
N_g	Rotational speed of the gyrational motion, rad. s^{-1}
N_p	Rotational speed of the planetary motion, rad. s^{-1}

Greek Symbols

$\vec{\omega}_i$	Angular velocity, rad. s^{-1}
α_1	Gyrational angle, rad
α_2	Planetary angle, rad

Superscripts & Subscripts

i	Particle i
j	Particle j
n	Normal
t	Tangential
g	Gyrational
p	Planetary
c	Contact
d	Damping

References

[1] M. C. Valigi and I. Gasperini, "Planetary vertical concrete mixers: Simulation and predicting useful life in steady states and in perturbed conditions," Simulation Modelling Practice and Theory, vol. 15, no. 10, pp. 1211–1223, Nov. 2007, doi: https://doi.org/10.1016/j.simpat.2007.07.010.

[2] B. Cazacliu, "In-mixer measurements for describing mixture evolution during concrete mixing," Chemical Engineering Research and Design, vol. 86, no. 12, pp. 1423–1433, Dec. 2008, doi: https://doi.org/10.1016/j.cherd.2008.08.021.

[3] M. C. Valigi, S. Logozzo, and M. Rinchi, "Wear resistance of blades in planetary concrete mixers. Design of a new improved blade shape and 2D validation," Tribology International, vol. 96, pp. 191–201, Apr. 2016, doi: https://doi.org/10.1016/j.triboint.2015.12.020.

[4] M. C. Valigi, S. Logozzo, and M. Rinchi, "Wear resistance of blades in planetary concrete mixers. Part II: 3D validation of a new mixing blade design and efficiency evaluation," Tribology International, vol. 103, pp. 37–44, Nov. 2016, doi: https://doi.org/10.1016/j.triboint.2016.06.040.

[5] J. Long et al., "Discrete element simulation for mixing performances and power consumption in a twin-blade planetary mixer with non-cohesive particles," Advanced Powder Technology, vol. 33, no. 2, pp. 103437–103437, Jan. 2022, doi: https://doi.org/10.1016/j.apt.2022.103437.

[6] J. Zheng et al., "Digital evaluation of planetary concrete mixer efficiency," Automation in Construction, vol. 150, p. 104834, Jun. 2023, doi: https://doi.org/10.1016/j.autcon.2023.104834.

[7] J. Salamat and B. Genç, "Mixing Performance Analysis of Cohesive Granular Particles in a Planetary Concrete Mixer Containing Two Different Mixing Units via DEM," Orclever Proceedings of Research and Development, vol. 3, no. 1, pp. 311–320, Dec. 2023, doi: https://doi.org/10.56038/oprd.v3i1.291.

[8] M. Poux, P. Fayolle, J. Bertrand, D. Bridoux, and J. Bousquet, "Powder mixing: Some practical rules applied to agitated systems," Powder Technology, vol. 68, no. 3, pp. 213–234, Dec. 1991, doi: https://doi.org/10.1016/0032-5910(91)80047-M.

[9] LIGGGHTS, LAMMPS Improved for General Granular and Granular Heat Transfer Simulations Retrieved from http://www.cfdem.com

[10] LAMMPS, LAMMPS User Manual, Sandia National Laboratories, USA. (Retrieved from http://lammps.sandia.gov/doc/Manual.html).

[11] P. A. Cundall and O. D. L. Strack, "A discrete numerical model for granular assemblies," Géotechnique, vol. 29, no. 1, pp. 47–65, Mar. 1979, doi: https://doi.org/10.1680/geot.1979.29.1.47.

[12] J. Salamat and B. Genç, "Numerical Simulation of Granular Flow in Concrete Batching Plant via Discrete Element Method," The European Journal of Research and Development, vol. 3, no. 2, pp. 11–28, May 2023, doi: https://doi.org/10.56038/ejrnd.v3i2.219.